2017 IEEE 56th Annual Conference on Decision and Control (CDC)
December 12-15, 2017, Melbourne, Australia

Community-level Geothermal Heat Pump System Management via an Aggregation-disaggregation Framework

Xuan Zhang, Bin Yan, Wenbo Shi, Ali Malkawi, Qing-Shan Jia and Na Li

Abstract— **This paper presents an aggregation-disaggregation framework for the community-level management of widely-used Geothermal Heat Pump (GHP) systems in energy efficient buildings. In accordance with the layered operating architecture of the current power grid, this framework operates at two different time-scales. At a slow time-scale, each building predicts its GHP system future power consumption information consisting of both upper and lower bounds and the utility function, using aggregate thermal zone information and short-term disturbance forecasts. The information is then reported to a control center, i.e., an aggregator for all GHP systems in the community who determines and notifies their future nominal consumptions. At a fast time-scale, a distributed control scheme is designed based on a primal-dual gradient method, such that the nominal consumption can be tracked as closely as possible under real disturbances, using only local measurements and neighboring communications. In general, our framework provides an approach to scaling up the optimization and control for zone-building-aggregator interaction, which can be used to provide flexible ancillary services from a population of GHP systems to support the power distribution/transmission systems.**

I. Introduction

Demand side management is becoming a key component in the current power grid that helps reduce peak load and adapt elastic demand to fluctuating generations [1]. Given the fact that Heating Ventilation and Air Conditioning (HVAC) systems in buildings account for 15%-20% of energy consumption worldwide [2], [3], HVAC systems have a great potential to provide ancillary services in demand side management. Thus, making them more active and responsive has drawn recent attention as a way to assist in improving grid reliability, efficiency, and robustness to uncertain generations.

Among different types of HVAC systems, Geothermal Heat Pump (GHP) systems are widely adopted due to their highly efficient use of energy. They can usually deliver more than 3kWh of heat with 1kWh of electricity [4]. Hence the main focus of this paper is on GHP systems. In order to achieve active and responsive GHP systems capable of providing ancillary services to the power grid, aggregation and coordination across a population of buildings are necessary, since the capability of the collective is much more dominant and helpful than each individual's. Although various control techniques have been developed for GHP systems [5]–[7], most of them are designed only to ensure the efficient and robust operation of the system in a single building. If merely scaling up them under the current operating architecture of the grid, large amounts of sensing, communication and computation will be required for grid operators to integrate the building GHP systems. Also, from the grid operators' viewpoint, it is expensive to interact with a large number of buildings, collecting every piece of information from and sending control commands to each system in real-time. Therefore, new optimization and control frameworks are desired as GHP system management schemes that can be seamlessly embedded into the current grid operation.

The major issue that the desired frameworks need to address is: the optimization and control of the power grid is hierarchical [8], namely, how should lower-level responsive GHP systems be included in a higher-level (e.g., communities, microgrids, distribution/transmission networks) power dispatch problem? In particular, (i) since each GHP system has its own dynamics and operating constraints whereas the higher-level operator is unable to collect all of them, which messages should each GHP system report to the higher-level operator, and how to compute them efficiently? (ii) Given a certain operating goal or signal from the higher-level operator, how to achieve that goal via properly controlling each GHP system, without violating the operating constraints? These questions lead to the imperative topic on aggregation and disaggregation of GHP (and general HVAC) systems.

In fact, some recent work has focused on aggregation and disaggregation of HVAC systems (more generally, Thermostatically Controlled Loads or TCLs) [9]–[13]. For example, a generalized battery model was developed to characterize the aggregate flexibility of TCLs in [9], and a direct load control architecture was proposed to track an automatic generation control signal from the system operator. In [10], a building-aggregator-grid interaction contract framework was presented based on Economic Model Predictive Control (MPC), which could effectively aggregate the flexible power consumption of a group of HVAC fans to serve as fast regulation reserve to the grid. In [11], an iterative pricing mechanism was designed based on mean-field games in order to steer TCLs to some desired aggregate behavior. In [12], the authors proposed a novel geometric approach to designing a virtual battery model for TCLs, in which the aggregate flexibility was characterized by the Minkowski sum of multiple homothetic polytopes. In [13], an adaptive, online state estimation and control method was proposed for large populations of TCLs subject to biased disturbances. However, most literatures have one or

This work was supported by the Department of Energy Advanced Research Projects Agency-Energy (ARPA-E) under the Network Optimized Distributed Energy Systems (NODES) program, Harvard Center for Green Buildings and Cities, and NSFC 61673229. X. Zhang, B. Yan, W. Shi and A. Malkawi are with Harvard Center for Green Buildings and Cities, 20 Sumner Road, Cambridge, MA 02138, USA (email: xuan_zhang@g.harvard.edu, {byan, wshi, amalkawi}@gsd.harvard.edu). Qing-Shan Jia is with Department of Automation, Tsinghua University, Beijing 100084, China (email: jiaqs@tsinghua.edu.cn). X. Zhang and N. Li are with the School of Engineering and Applied Sciences, Harvard University, 29 Oxford Street, Cambridge, MA 02138, USA (email: nali@seas.harvard.edu).

more of the following drawbacks: (i) the thermal model of buildings and HVAC systems is linear, and/or does not capture temperature dynamics of individual thermal zones; (ii) the aggregate information that buildings provide to the higher-level operator does not include the utility function, which is important for the higher-level operator to make any decision [14]; (iii) the control scheme for the HVAC system is implemented in a centralized manner that requires lots of sensing, communication, computation, and may need measurement of disturbances, e.g., indoor heat gains, which are hard to obtain.

Contribution of the paper. This paper aims to develop an aggregation-disaggregation framework for the management of building GHP systems at the community level. Specifically, we demonstrate how convex optimization assists in the related computation and control. We consider nonlinear thermal dynamics with practical operating constraints of GHP systems. We focus on zone-building-community interaction, in which the GHP system consumption flexibility, including the utility function, is characterized through computationally efficiently solving proper optimization problems. In addition, we design a distributed controller for zone-level control such that the operating signal from the higher-level operator can be tracked as closely as possible by each GHP system with only local measurements (without measuring any real disturbance) and neighboring communications.

Nomenclature and Notation: In this paper, $\mathcal{G}_F$ denotes the set of buildings equipped with a GHP system for Floor heating/cooling, and $\mathcal{G}_F(b)$ is the set of thermal zones/rooms of building b in $\mathcal{G}_F$. $\mathcal{G}_R$ is the set of buildings equipped with a GHP system for Radiator heating/cooling, and $\mathcal{G}_R(b)$ is the set of zones of building b in $\mathcal{G}_R$. $\mathcal{N}(i)$ denotes the set of neighboring zones of zone i. $\dot{x} = \dot{x}(t)$ denotes the derivative of a state variable $x(t)$ with respect to time t, i.e., $\dot{x}(t) = \frac{d}{dt}x(t)$. The positive projection of a function $h(y)$ on a variable $x \in [0, +\infty)$, $(h(y))_x^+$ is:

$$(h(y))_x^+ = \begin{cases} h(y) & \text{if } x > 0 \\ \max(0, h(y)) & \text{if } x = 0 \end{cases}.$$

II. Problem Setup

In this section, we first present the configuration of the building GHP system and its thermal dynamics. Then we introduce the aggregation-disaggregation framework which is applicable to general thermal/HVAC systems.

A. GHP system in buildings

The schematic of a typical GHP system is illustrated in Figure 1, which consists of two hydronic circuits, and one refrigerant circuit/the *heat pump*, interconnected by two heat exchangers, i.e., an evaporator and a condenser [4], [7]. In winter, it transfers heat from the underground soil/water to buildings for heating, and vice versa in summer for cooling. The heat/cold can be either distributed to building concrete floors (i.e., floor heating/cooling) or hydronic radiators (i.e., radiator heating/cooling). Detailed working process of the GHP system is available in [15]. In the following, we will use *floor heating* as an example to demonstrate the aggregation-disaggregation procedure, while radiator heating is similar and will be reported briefly. On the other hand, although the

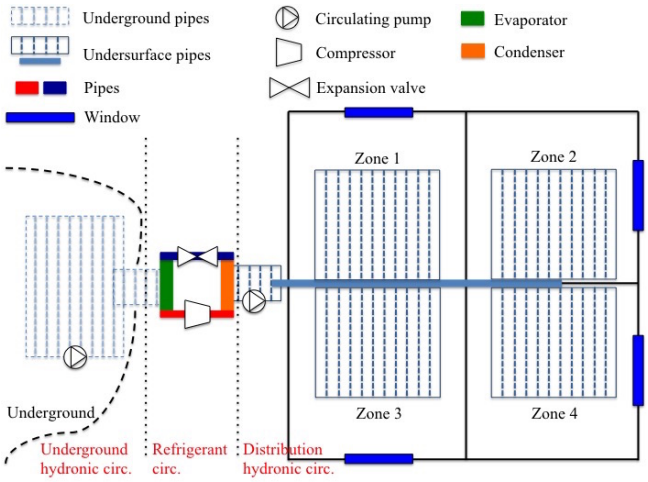

Fig. 1: Schematic of a typical GHP system.

cooling mode is less commonly used, the related aggregation-disaggregation follows the same procedure. For brevity, we only focus on the *heating mode* case in this paper.

In general, the heat pump consumes electric power to transfer heat to the water in the distribution hydronic circuit. The amount of this heat depends on water flow rate, heat pump supply/forward temperature, and return water temperature [7], [16]. Each zone in the building is equipped with a Thermal Wax Actuator (TWA) that adjusts the valve opening of the pipes for regulating the flow rate. The supply temperature is adjusted by regulating the compressor of the heat pump. The return water temperature can be approximated by the floor/radiator temperature which is accurate enough for control design [17].

B. Thermal dynamic model with a GHP system

The thermal dynamic model for each zone in a building with floor heating is described by a reduced Resistance-Capacitance (RC) model [18] (more discussion on this model is available in [15], [19]):

$$C_i\dot{T}_i = \frac{T^o - T_i}{R_i} + \sum_{j\in\mathcal{N}(i)} \frac{T_j - T_i}{R_{ij}} + \frac{T_{fi} - T_i}{R_{afi}} + Q_i \quad (1)$$

where $i \in \mathcal{G}_F(b), b \in \mathcal{G}_F$, C_i is the thermal capacitance, T_i is the indoor temperature, T^o is the outdoor temperature, R_i is the thermal resistance of the wall and window separating zone i and outside, $R_{ij} = R_{ji}$ is the thermal resistance of the wall separating zones i and j, T_{fi} is the floor temperature, R_{afi} is the thermal resistance between the indoor air and the floor, and Q_i is the heat gain from exogenous sources (e.g., user activity, solar radiation and device operation).

The thermal dynamics of floors equipped with a GHP system is given by a simplified lumped element model [7]

$$C_{fi}\dot{T}_{fi} = \frac{T_i - T_{fi}}{R_{afi}} + \frac{T_{wi} - T_{fi}}{R_{fwi}} \quad (2a)$$

$$C_{wi}\dot{T}_{wi} = \frac{T_{fi} - T_{wi}}{R_{fwi}} + c_w q_i (T_b^s - T_{fi}) \quad (2b)$$

where $i \in \mathcal{G}_F(b), b \in \mathcal{G}_F$, C_{fi} is the thermal capacitance of the floor, T_{wi} is the temperature of the water in pipes, R_{fwi}

is the thermal resistance between the floor and the water, C_{wi} is the thermal capacitance of the water, c_w is the specific heat of the water, q_i is the water flow rate, and T_b^s is the supply temperature of the heat pump. It is a standard operation that T_b^s is a common input to the whole building [7]. But the input q_i is adjusted differently for different zones.

The electric power consumption of the GHP system of the building equals the consumption of the heat pump, i.e.,

$$p_b = \sum\nolimits_{i\in\mathcal{G}_F(b)} c_w q_i (T_b^s - T_{fi})/(-a_b T_b^s + b_b) \quad (3)$$

where $-a_b T_b^s + b_b > 0$ is the Coefficient of Performance (COP, i.e., the ratio of the produced heat to the consumed electricity) of the heat pump, and $\sum_{i\in\mathcal{G}_F(b)} c_w q_i (T_b^s - T_{fi})$ is the produced heat[1]. The COP has been approximated as a linear function of T_b^s [16], and a_b, b_b are positive coefficients obtained from the heat pump data sheet [7], [16].

The thermal dynamics of a building equipped with a GHP system for radiator heating is similar to (1)-(2), including a reduced RC model and a simplified lumped element model,

$$C_i \dot{T}_i = \frac{T^o - T_i}{R_i} + \sum_{j\in\mathcal{N}(i)} \frac{T_j - T_i}{R_{ij}} + \frac{T_{ri} - T_i}{R_{ari}} + Q_i \quad (4a)$$

$$C_{ri} \dot{T}_{ri} = \frac{T_i - T_{ri}}{R_{ari}} + c_w q_i (T_b^s - T_{ri}) \quad (4b)$$

where $i \in \mathcal{G}_R(b), b \in \mathcal{G}_R$, T_{ri} is the temperature of the radiator combined with inside water, R_{ari} is the thermal resistance between the indoor air and the radiator, and C_{ri} is the thermal capacitance of the radiator. The electric power consumption of the GHP system is the same as (3) with $\sum_{i\in\mathcal{G}_F(b)} c_w q_i (T_b^s - T_{fi})$ changing to $\sum_{i\in\mathcal{G}_R(b)} c_w q_i (T_b^s - T_{ri})$. Note that floor heating and radiator heating can exist in the same building in different zones.

C. The Aggregation-disaggregation framework

The operating structure of our aggregation-disaggregation framework for building thermal system management in communities is illustrated in Figure 2. This framework operates at two different time-scales. At a slow time-scale, e.g., 5-15 minutes, each thermal zone in buildings firstly uses forecasts and historical data to predict future disturbances, e.g., the outdoor temperature and indoor heat gains, which are usually *step change and slow-varying within a short period of time*. Secondly, each building *aggregates* information from all its thermal zones to calculate (i) the system future power consumption range consisting of the upper and lower power consumption bounds $[\underline{p}_b, \overline{p}_b]$, as well as (ii) the future utility function of the system $U_b(p_b)$ with respect to the consumption $p_b \in [\underline{p}_b, \overline{p}_b]$. Then each building reports its future consumption information to a control center – an aggregator in charge of all thermal systems in the community. Based on the received information, the control center determines the nominal consumption p_b^* for each building and sends the values back to them[2]. At a fast time-scale, each building carries out *distributed/decentralized* control to guide every controllable component, q_i, T_b^s in this paper, of the thermal system to appropriately adapt their behavior such that the given nominal value p_b^* can be tracked as closely as possible without affecting user comfort. This is called the *disaggregation* procedure.

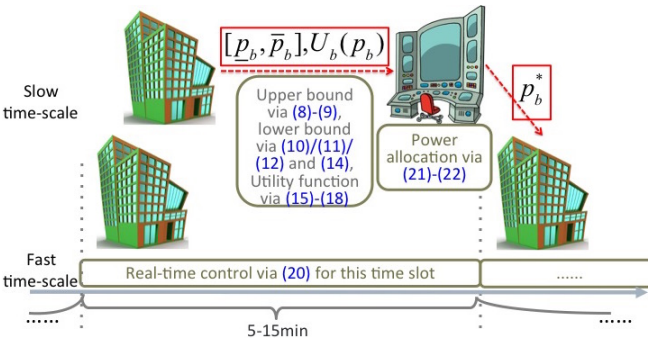

Fig. 2: The operating structure of the proposed framework.

The reasons to adopt the time-scale separation in our framework include: (i) it conforms with the hierarchical optimization and control architecture in current power systems so that our framework can be easily embedded into it; (ii) the rate of changes in disturbances is much slower than that of control actuators in the thermal system, due to which the operation planning/aggregation and real-time control/disaggregation can be separated.

III. Aggregation in Buildings with GHP Systems

A. Steady-state aggregation

In this paper, we consider steady-state aggregation which requires only short-term prediction, less communication and computation compared with multi-step aggregation [20], and thus is easy to implement. The reasons are as follows. During a short period of time, e.g., 5-15 minutes, the outdoor temperature T^o and the indoor heat gain Q_i vary slowly and are within certain ranges. Under slowly-varying exogenous inputs T^o and Q_i, the GHP system can quickly (compared with the speed of changes in disturbances) drive the temperature in each zone to stay at or closely to some steady state, which satisfies user comfort and system operating constraints given by Equation (5c)-(5e) listed below. Based on this fact, each building can predict its GHP system future power consumption information (consisting of the range and the utility function) via steady-state aggregation with short-term prediction of disturbances. To avoid confusion between the steady-state values and temperature dynamics, we use $Z_\bullet$ to denote the steady-state temperature value of a corresponding state $T_\bullet$ (remark that $T_\bullet$ is the temperature resulting from model (1)-(2) or (4)). Also, a variable with tilde, i.e., $\tilde{\bullet}$, denotes its predicted value.

Under short-term prediction and normal operation, when the dynamics (1)-(2) or (4) reach steady state, we have

Steady-state equation

$$\frac{\tilde{T}^o - Z_i}{R_i} + \sum_{j\in\mathcal{N}(i)} \frac{Z_j - Z_i}{R_{ij}} + \frac{Z_{fi} - Z_i}{R_{afi}} + \tilde{Q}_i = 0 \quad (5a)$$

[1]In the heating mode, $T_b^s > T_{fi}, \forall i$ holds; in the cooling mode, $T_b^s < T_{fi}, \forall i$ holds. This is always true in practice [7], [16].

[2]We do not limit the way how the control center determines the nominal values. For instance, the control center can aggregate the information from individual buildings to participate in the electricity market.

$$\frac{Z_i - Z_{fi}}{R_{afi}} + c_w q_i (T_b^s - Z_{fi}) = 0 \tag{5b}$$

User comfort

$$\underline{T}_i \le Z_i \le \overline{T}_i \tag{5c}$$

GHP system operating constraint

$$0 \le q_i \le \overline{q}_i \tag{5d}$$

$$\underline{T}_b^s \le T_b^s \le \overline{T}_b^s \tag{5e}$$

Prediction uncertainty

$$\underline{T}^o \le \tilde{T}^o \le \overline{T}^o \tag{5f}$$

$$\underline{Q}_i \le \tilde{Q}_i \le \overline{Q}_i \tag{5g}$$

where $i \in \mathcal{G}_F(b), b \in \mathcal{G}_F$, (5b) results from the steady state equation of (2), and the system operating constraints (5d)-(5e) are in accord with those in the optimization problem (7) in [7]. In reality, the disturbance predictions are within certain ranges, which is why we introduce (5f)-(5g). Moreover, we introduce $\tilde{T}^{om} \in [\underline{T}^o, \overline{T}^o], \tilde{Q}_i^m \in [\underline{Q}_i, \overline{Q}_i]$ as the most likely predicted (average) values of $\tilde{T}^o, \tilde{Q}_i$: if not provided, the default values are $\tilde{T}^{om} = (\underline{T}^o + \overline{T}^o)/2, \tilde{Q}_i^m = (\underline{Q}_i + \overline{Q}_i)/2$. These parameters will be used to seek a proper utility function later. For the case of using radiator heating, the related equation is similar. Equation (5) actually defines a region for system future steady states. *Here we assume that this region is feasible, and in particular, it is feasible when* $\tilde{T}^o = \tilde{T}^{om}, \tilde{Q}_i = \tilde{Q}_i^m$ *hold*: if the region is empty, users could relax their comfort ranges (5c) to guarantee the feasibility of (5).

B. The upper bound

Let $\overline{u}_b = \sum_{i \in \mathcal{G}_F(b)} c_w q_i (T_b^s - Z_{fi})$, i.e., the produced heat from the GHP system, and $u_i = c_w q_i (T_b^s - Z_{fi}), i \in \mathcal{G}_F(b)$. Finding the upper bound of p_b is equivalent to solving the following optimization problem:

$$\max_{Z_i, Z_{fi}, u_i, T_b^s, \overline{u}_b, \tilde{T}^o, \tilde{Q}_i} \frac{\overline{u}_b}{b_b - a_b T_b^s} \tag{6a}$$

$$\text{s. t.} \quad \text{(5a), (5c), (5e)-(5g)} \tag{6b}$$

$$\frac{Z_i - Z_{fi}}{R_{afi}} + u_i = 0 \tag{6c}$$

$$0 \le u_i \le c_w \overline{q}_i (T_b^s - Z_{fi}) \tag{6d}$$

$$\overline{u}_b = \sum\nolimits_{i \in \mathcal{G}_F(b)} u_i \tag{6e}$$

where $i \in \mathcal{G}_F(b), b \in \mathcal{G}_F$. However, the above problem is nonconvex since the objective function (6a) is nonconvex in the decision variables. Instead, we consider a modified version of this problem given by

$$\max_{Z_i, Z_{fi}, u_i, \overline{u}_b, \tilde{T}^o, \tilde{Q}_i, \underline{T}_b^s \le T_b^s \le \overline{T}_b^s} \frac{\overline{u}_b}{b_b - a_b T_b^s} \tag{7a}$$

$$\text{s. t.} \quad \text{(5a), (5c), (5f)-(5g), (6c), (6e)} \tag{7b}$$

$$0 \le u_i \le c_w \overline{q}_i (\overline{T}_b^s - Z_{fi}) \tag{7c}$$

where we have enlarged the constraint set by replacing (6d) with (7c). Because the decision variable T_b^s only appears in the objective function of (7) with the boundary constraint $\underline{T}_b^s \le T_b^s \le \overline{T}_b^s$ and does not affect the other constraints (7b)-(7c), solving problem (7) is equivalent to solving

$$\max_{Z_i, Z_{fi}, u_i, \overline{u}_b, \tilde{T}^o, \tilde{Q}_i} \frac{\overline{u}_b}{b_b - a_b \overline{T}_b^s} \tag{8a}$$

$$\text{s. t.} \quad \text{(7b)-(7c).} \tag{8b}$$

The following result shows the relation between (6) and (8).

Theorem 1. *The optimal objective function values of problems (6) and (8) are the same.*

Proof. It is sufficient to show that the optimal objective function values of (6) and (7) are the same. Because the constraint set of (6) is a subset of that of (7), the optimal objective function value of (6) is no more than that of (7). On the other hand, by setting $T_b^s = \overline{T}_b^s$ in (6), this problem exactly becomes (8) which is equivalent to (7). Thus, the optimal objective function value of (6) is the same as that of (7), and is achieved when $T_b^s = \overline{T}_b^s$. □

By solving the linear programming problem (8), the upper bound of electric power consumption of the GHP system is

$$\overline{p}_b = \overline{u}_b^* / (b_b - a_b \overline{T}_b^s) \tag{9}$$

where $\overline{u}_b^*$ is the optimal solution of (8).

C. The lower bound

As before, finding the lower bound of p_b is equivalent to solving the following optimization problem:

$$\min_{Z_i, Z_{fi}, u_i, T_b^s, \underline{u}_b, \tilde{T}^o, \tilde{Q}_i} \frac{\underline{u}_b}{b_b - a_b T_b^s} \tag{10a}$$

$$\text{s. t.} \quad \text{(5a), (5c), (5e)-(5g), (6c)-(6d)} \tag{10b}$$

$$\underline{u}_b = \sum\nolimits_{i \in \mathcal{G}_F(b)} u_i \tag{10c}$$

which is nonconvex as the objective function (10a) is nonconvex in the decision variables. Note that now we can not apply the method of exactly convexfying (6) as (8) to the above problem. But we can use this method to obtain two approximate versions of problem (10), which provide an aggressive lower bound and a conservative lower bound:

$$\min_{Z_i, Z_{fi}, u_i, \underline{u}_b, \tilde{T}^o, \tilde{Q}_i} \frac{\underline{u}_b}{b_b - a_b \underline{T}_b^s} \tag{11a}$$

$$\text{s. t.} \quad \text{(5a), (5c), (5e)-(5g), (6c), (10c)} \tag{11b}$$

$$0 \le u_i \le c_w \overline{q}_i (\overline{T}_b^s - Z_{fi}) \tag{11c}$$

for an aggressive (i.e., smaller) lower bound, and

$$\min_{Z_i, Z_{fi}, u_i, \underline{u}_b, \tilde{T}^o, \tilde{Q}_i} \frac{\underline{u}_b}{b_b - a_b \underline{T}_b^s} \tag{12a}$$

$$\text{s. t.} \quad \text{(5a), (5c), (5e)-(5g), (6c), (10c)} \tag{12b}$$

$$0 \le u_i \le c_w \overline{q}_i (\underline{T}_b^s - Z_{fi}) \tag{12c}$$

for a conservative (i.e., larger) lower bound. Remark that (11) is feasible since (10) is feasible, while (12) may be infeasible. By assuming that problems (10), (11) and (12) are all feasible, we have the following theorem.

Theorem 2. *The optimal objective function values of prob-*

lems (10), (11) and (12) satisfy

$$\frac{\underline{u}_b^{(12)*}}{b_b - a_b \underline{T}_b^s} \geq \frac{\underline{u}_b^{(10)*}}{b_b - a_b T_b^{s(10)*}} \geq \frac{\underline{u}_b^{(11)*}}{b_b - a_b \underline{T}_b^s} \tag{13}$$

where the optimal solutions of those problems are marked with problem number and $*$.

Proof. The proof is similar to that of Theorem 1 by studying the inclusion relation between the constraint sets of those optimization problems, and thus is omitted for brevity. □

Each building solves either the nonconvex problem (10) for an exact lower bound, or the linear programming problem (11)/(12) for an approximate lower bound, i.e.,

$$\underline{p}_b = \underline{u}_b^* / (b_b - a_b T_b^{s*}) \tag{14}$$

where $\underline{u}_b^*, T_b^{s*}$ is the optimal solution of (10)/(11)/(12), and $T_b^{s*} = \underline{T}_b^s$ when solving (11)/(12) for $\underline{p}_b$.

D. The most likely consumption and the utility function

Let the temperature set point determined by users be $T_i^{set} \in (\underline{T}_i, \overline{T}_i)$: if a user does not specify the set point, then $T_i^{set} = (\underline{T}_i + \overline{T}_i)/2$. It is straightforward that the most likely/desired consumption of the GHP system p_b^d is the value at which user comfort inside the building is maximumly guaranteed, and meanwhile, the COP is as high as possible for system energy efficiency (equivalently, the heat pump supply temperature needs to be low). So we consider the following optimization problem for seeking p_b^d:

$$\min_{Z_i, Z_{fi}, u_i, T_b^s} \sum_{i \in \mathcal{G}_F(b)} \frac{\phi_i}{2}(Z_i - T_i^{set})^2 + \frac{\phi_b}{2}(T_b^s - \underline{T}_b^s)^2 \tag{15a}$$

$$\text{s. t.} \quad \text{(5a), (5c), (5e), (6c)-(6d)} \tag{15b}$$

$$\tilde{T}^o = \tilde{T}^{om},\ \tilde{Q}_i = \tilde{Q}_i^m \tag{15c}$$

where ϕ_i, ϕ_b are nonnegative weight coefficients representing the priority of zones as well as optimizing the COP. The reason to fix $\tilde{T}^o, \tilde{Q}_i$ to be their most likely values is that they are not controllable inputs so that they should not be actively tuned to seek the most likely consumption (on the contrary, we do not fix them when seeking the upper and lower bounds since doing so results in a larger set $[\underline{p}_b, \overline{p}_b]$, which can provide more flexibility for the control center to make a power allocation plan among buildings). By solving the convex optimization problem (15), the most likely electric power consumption of the GHP system is given by

$$p_b^d = \sum\nolimits_{i \in \mathcal{G}_F(b)} u_i^* / (b_b - a_b T_b^{s*}) \tag{16}$$

where u_i^*, T_b^{s*} is the optimal solution of (15).

Clearly, $p_b^d \in [\underline{p}_b, \overline{p}_b]$ is always true. Once the most likely consumption is obtained, each building uses $[\underline{p}_b, \overline{p}_b], p_b^d$ to generate its GHP system future utility function which will be sent to the control center. An example is the quadratic utility function given by $U_b(p_b) = -\frac{1}{2}(p_b - p_b^d)^2, p_b \in [\underline{p}_b, \overline{p}_b]$. In fact, it is an interesting direction to consider how to formulate proper utility functions with the predicted information. Due to the space limit, we only propose a simple approach via quadratic curve fitting, considering efficiency loss, rather than using $U_b(p_b) = -\frac{1}{2}(p_b - p_b^d)^2, p_b \in [\underline{p}_b, \overline{p}_b]$.

Let $EL_b(p_b)$ be the optimal objective function value of the following convex optimization problem:

$$\min_{Z_i, Z_{fi}, u_i, T_b^s} \frac{1}{\sum_{i \in \mathcal{G}_F(b)} \phi_i + \phi_b + \psi_b} \Bigg[\sum_{i \in \mathcal{G}_F(b)} \frac{\phi_i}{2}(Z_i - T_i^{set})^2 + \frac{\phi_b}{2}(T_b^s - \underline{T}_b^s)^2 + \frac{\psi_b}{2}\Big(\sum\nolimits_{i \in \mathcal{G}_F(b)} u_i - p_b(b_b - a_b T_b^s) \Big)^2 \Bigg] \tag{17a}$$

$$\text{s. t.} \quad \text{(15b)-(15c)} \tag{17b}$$

where p_b is given, and ψ_b is a nonnegative weight coefficient representing the priority of tracking the point p_b. The meaning of $EL_b(p_b)$ is the Efficiency Loss for a given nominal consumption p_b, considering user comfort, optimizing the COP and consumption tracking (i.e., a convex combination of these indexes). It is true that $EL_b(p_b^d) \leq EL_b(p_b), \forall p_b \in [\underline{p}_b, \overline{p}_b]$ since the optimal solution of problem (15) satisfies $\sum_{i \in \mathcal{G}_F(b)} u_i^* = p_b^d(b_b - a_b T_b^{s*})$. We next compute $EL_b(\underline{p}_b)$ and $EL_b(\overline{p}_b)$, and finally use the information to fit a quadratic utility function given by

$$U_b(p_b) = \alpha_b p_b^2 + \beta_b p_b + \gamma_b \tag{18a}$$

$$U_b(p_b^d) = -EL_b(p_b^d), U_b(\underline{p}_b) = -EL_b(\underline{p}_b), \quad U_b(\overline{p}_b) = -EL_b(\overline{p}_b). \tag{18b}$$

Note that we can also use more points in $[\underline{p}_b, \overline{p}_b]$ to fit a quadratic or higher order polynomial utility function.

Remark 1. *In the aggregation procedure, we have assumed that the predicted disturbances are within certain bounds. However, the real disturbances may still violate the predicted bounds in reality, i.e., there may still be prediction errors. These errors may cause infeasibility in the disaggregation procedure if the real disturbances deviate too much from the predicted ones. Thus, the accuracy of the prediction matters. One way to overcome the infeasibility issue could be tuning user comfort constraint (5c). In the simulation section, the prediction accuracy is within $\pm 2^\circ C$ and $\pm 20\%$, and this does not cause any infeasibility in the disaggregation procedure.*

For the case of using radiator heating, seeking related consumption information follows the same procedure.

IV. Disaggregation via Real-time Distributed Control

Once the future consumption range $[\underline{p}_b, \overline{p}_b]$ and the utility function of the GHP system $U_b(p_b)$ are obtained, each building sends the information to the control center. After making a power allocation decision for the next time slot (examples are provided in the Appendix), the control center notifies each building the nominal operating point p_b^*. When the new time slot begins, the thermal system regulates its controllable inputs (i.e., q_i, T_b^s of the GHP system) so that p_b^* can be tracked as closely as possible under real disturbances (in addition, optimizing user comfort and the COP as shown in the objective function (17a) can also be included). The goal of disaggregation is to design control inputs to drive system (1)-(2) or (4) to an appropriate steady state which achieves the aforementioned purpose. In this section, we

propose a disaggregation formulation (i.e., a steady-state optimization problem formulation), which then leads to a distributed control scheme for the GHP system.

Consider the steady-state optimization problem given by

$$\min_{Z_i,,u_i,T_b^s} \sum_{i\in\mathcal{G}_F(b)} \frac{\phi_i}{2}(Z_i - T_i^{set})^2 + \frac{\phi_b}{2}(T_b^s - \underline{T}_b^s)^2 + \frac{\psi_b}{2}\Big(\sum\nolimits_{i\in\mathcal{G}_F(b)} u_i - p_b^*(b_b - a_b T_b^s)\Big)^2 \quad (19a)$$

$$\text{s. t.} \quad (5c),\ (5e) \quad (19b)$$

$$\frac{T^o - Z_i}{R_i} + \sum_{j\in\mathcal{N}(i)} \frac{Z_j - Z_i}{R_{ij}} + u_i + Q_i = 0 \quad (19c)$$

$$0 \le u_i \le c_w \overline{q}_i (T_b^s - Z_i)/(1 + c_w \overline{q}_i R_{afi}) \quad (19d)$$

where we have used $Z_{fi} = Z_i + R_{afi} u_i$ from equation (6c) so that now the problem is independent of Z_{fi}, and T^o, Q_i are real disturbances. Assume that problem (19) is feasible and satisfies Slater's constraint qualification [21]. Then (19) can be solved via convex optimization techniques. Once the optimal solution is derived, the optimal control input q_i^* is obtained as $q_i^* = u_i^*/(c_w(T_b^{s*} - Z_i^* - R_{afi}u_i^*))$.

Problem (19) can be solved in either a centralized or distributed/decentralized way. Any centralized algorithm requires measuring the outdoor temperature T^o and the indoor heat gain Q_i in every zone. Because these exogenous disturbances can fluctuate and can be hard to measure, the cost of centralized algorithms would be expensive. Next we develop a real-time distributed algorithm that does not need measurement of these disturbances based on [15]:

$$\dot{Z}_i = k_{Z_i}\Big(\phi_i(T_i^{set} - Z_i) - \sum_{j\in\mathcal{N}(i)} \frac{k_{\zeta_j}(\zeta_j + C_j T_j)}{R_{ij}} + k_{\zeta_i}(\zeta_i + C_i T_i)\Big(\frac{1}{R_i} + \sum_{j\in\mathcal{N}(i)} \frac{1}{R_{ij}}\Big) - \nu_i^+ + \nu_i^- - \mu_i^+ c_w \overline{q}_i/(1 + c_w \overline{q}_i R_{afi})\Big) \quad (20a)$$

$$\dot{u}_i = k_{u_i}\Big(\psi_b\Big(p_b^*(b_b - a_b T_b^s) - \sum_{i\in\mathcal{G}_F(b)} u_i\Big) - \zeta_i - \mu_i^+ + \mu_i^- + k_{eu_i}(\hat{u}_i - u_i)\Big) \quad (20b)$$

$$\dot{\hat{u}}_i = \hat{k}_{eu_i}(u_i - \hat{u}_i) \quad (20c)$$

$$\dot{T}_b^s = k_{T_b^s}\Big(\psi_b p_b^* a_b\Big(p_b^*(b_b - a_b T_b^s) - \sum_{i\in\mathcal{G}_F(b)} u_i\Big) - \epsilon_b^+ + \epsilon_b^- + \phi_b(\underline{T}_b^s - T_b^s) + \sum_{i\in\mathcal{G}_F(b)} \frac{\mu_i^+ c_w \overline{q}_i}{1 + c_w \overline{q}_i R_{afi}}\Big) \quad (20d)$$

$$\dot{\zeta}_i = \frac{T_i - Z_i}{R_i} + \sum_{j\in\mathcal{N}(i)} \frac{T_i - Z_i - T_j + Z_j}{R_{ij}} + u_i + \frac{T_i - T_{fi}}{R_{afi}} \quad (20e)$$

$$\dot{\nu}_i^+ = k_{\nu_i^+}(Z_i - \overline{T}_i)^+_{\nu_i^+}, \qquad \dot{\nu}_i^- = k_{\nu_i^-}(\underline{T}_i - Z_i)^+_{\nu_i^-} \quad (20f)$$

$$\dot{\mu}_i^+ = k_{\mu_i^+}(u_i - c_w \overline{q}_i (T_b^s - Z_i)/(1 + c_w \overline{q}_i R_{afi}))^+_{\mu_i^+}$$

$$\dot{\mu}_i^- = k_{\mu_i^-}(-u_i)^+_{\mu_i^-} \quad (20g)$$

$$\dot{\epsilon}_b^+ = k_{\epsilon_b^+}(T_b^s - \overline{T}_b^s)^+_{\epsilon_b^+}, \qquad \dot{\epsilon}_b^- = k_{\epsilon_b^-}(\underline{T}_b^s - T_b^s)^+_{\epsilon_b^-} \quad (20h)$$

$$\dot{q}_i = k_{q_i}(u_i/(c_w(T_b^s - Z_i - R_{afi}u_i)) - q_i) \quad (20i)$$

where $i \in \mathcal{G}_F(b), b \in \mathcal{G}_F$, $k_{\zeta_i}(\zeta_i + C_i T_i), \nu_i^+, \nu_i^-, \mu_i^+, \mu_i^-$, $\epsilon_b^+, \epsilon_b^-$ are the Lagrange multipliers/dual variables for constraints (19b)-(19d), $k_{Z_i}, k_{u_i}, k_{eu_i}, \hat{k}_{eu_i}, k_{T_b^s}, k_{\zeta_i}, k_{\nu_i^+}, k_{\nu_i^-}$, $k_{\mu_i^+}, k_{\mu_i^-}, k_{\epsilon_b^+}, k_{\epsilon_b^-}, k_{q_i}$ are positive scalars representing the controller gains. Note that (i) ζ_i is equivalent to $\tilde{\zeta}_i$ in Section III-B in [15], (ii) $\hat{u}_i$ is introduced to improve the performance of the controller as in [22], [23], and (iii) a low pass dynamics is adopted for q_i in (20i) to attenuate high frequency noises as in [19]. Now using (20d) and (20i) as the input to (1)-(2), we obtain a real-time distributed controller to regulate (1)-(2) to a steady state which is the optimal solution to (19).

Theorem 3. *Given constant/step change/slow-varying T^o, Q_i, each trajectory of the overall system (1)-(2) and (20) asymptotically converges to an equilibrium point at which $T_i = Z_i, u_i = c_w q_i (T_b^s - T_{fi}), T_b^s$ of this point is the optimal solution of (19).*

Proof. The proof is similar to that of Theorems 1 and 2 in [15], and thus is omitted for brevity. □

This theorem requires T^o, Q_i to be either constant, step change, or slow-varying, which holds in practice as they vary at a time-scale of minutes. Remark that controller (20) operates in real-time, i.e., at a time-scale of seconds.

Implementation. The proposed control scheme is completely distributed and can be implemented as follows. Given $C_i, R_i, R_{ij}, R_{afi}, \phi_i, \overline{q}_i$, each zone in the building collects $[\underline{T}_i, \overline{T}_i], T_i^{set}$ from users, measures its local indoor temperature T_i and floor temperature T_{fi}, receives the feedback signals $k_{\zeta_j}(\zeta_j + C_j T_j), T_j - Z_j$ from its neighboring zones and $T_b^s, \psi_b(p_b^*(b_b - a_b T_b^s) - \sum_{i\in\mathcal{G}_F(b)} u_i)$ from the compressor, and then uses the information to update $Z_i, u_i, \hat{u}_i, \zeta_i, \nu_i^+, \nu_i^-, \mu_i^+, \mu_i^-, q_i$. On the other hand, given $\phi_b, \psi_b, p_b^*, a_b, b_b, [\underline{T}_b^s, \overline{T}_b^s]$, the compressor receives the feedback signals $u_i, \mu_i^+ c_w \overline{q}_i/(1 + c_w \overline{q}_i R_{afi})$ from each zone, updates $T_b^s, \epsilon_b^+, \epsilon_b^-$, and then broadcasts $T_b^s, \psi_b(p_b^*(b_b - a_b T_b^s) - \sum_{i\in\mathcal{G}_F(b)} u_i)$. Here $C_i, R_i, R_{ij}, R_{afi}, \overline{q}_i, a_b, b_b, \underline{T}_b^s, \overline{T}_b^s$ are building parameters, ϕ_i, ϕ_b, ψ_b are specified by users, and p_b^* is from the control center. *Note that (20) is a dynamic feedback controller that adapts to changes in exogenous inputs (disturbances and the nominal point), and it is implemented in a much easier way than controllers based on MPC [4], [6], [7], [24].* Finally, the disaggregation for radiator heating systems follows the same procedure.

V. A Numerical Example

In this section, we present a numerical example on aggregation and disaggregation of three GHP systems in the same area (we do not add more buildings since our methods are scalable and this is already enough to show the effectiveness of the proposed framework). The configuration is: Building 1 consists of 3 zones with a triangle topology, all using radiator heating; Building 2 consists of 4 zones with a rectangle topology as in Figure 1, all using floor heating; Building 3 is the same as Building 2, with Zones 1-2 using floor heating and Zones 3-4 using radiator heating. The parameters of the simulation are from [15] with some random variations. Due

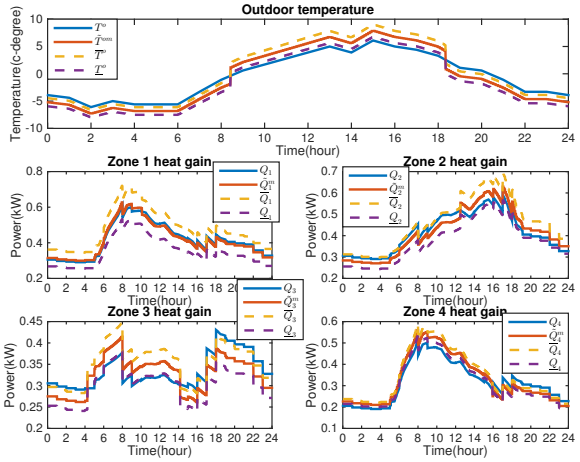

Fig. 3: Exogenous disturbances: predicted and real values.

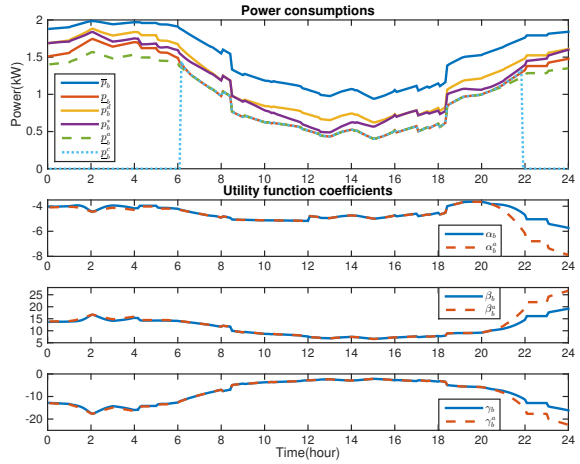

Fig. 4: Power consumption information via aggregation (superscripts 'a' and 'c' denote the cases of using (11) and (12) for lower bounds respectively).

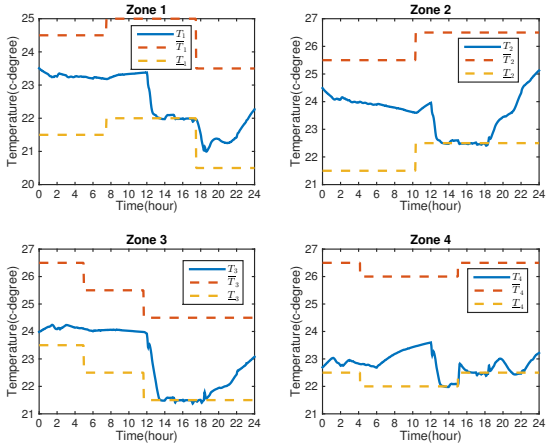

Fig. 5: Disaggregation: trajectories of zone temperatures.

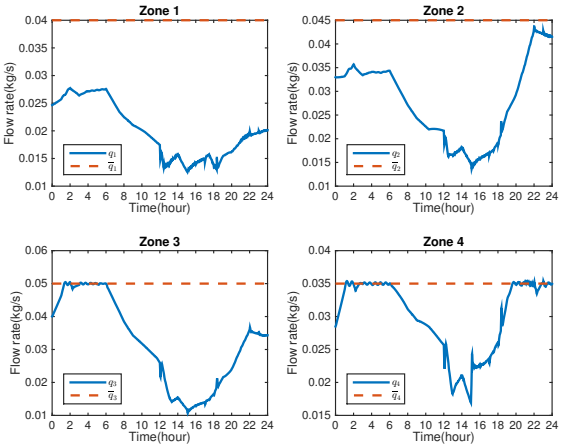

Fig. 6: Disaggregation: trajectories of flow rates.

to the space limit, we only show the result of Building 3 here (the weight coefficients are $\phi_i = 0.025, \phi_b = 0.01$, $\psi_b = 0.05$ before 12h and $\psi_b = 2.5$ thereafter).

In the aggregation procedure, assume that (i) the prediction accuracy of disturbances is within $\pm 2°$C and $\pm 20\%$ of their real values, as shown in Figure 3, (ii) the prediction of the outdoor temperature is the same for all buildings, and (iii) set points are the average of their upper and lower bounds as given in Figure 5. The aggregation result is illustrated in Figure 4, in which $\underline{p}_b^c = 0$ means that (12) is infeasible as mentioned earlier. We see that the future utility functions are always concave due to $EL_b(p_b^d) \leq EL_b(p_b), \forall p_b \in [\underline{p}_b, \overline{p}_b]$. In the simulation, the control center makes power allocation plans independently under a time-varying power capacity constraint (21c) in the Appendix to maximize the sum of utility functions derived with exact lower bounds. The nominal consumption of Building 3 is given by the purple curve p_b^* in Figure 4. *Remark that these figures demonstrate the results for* 24 *hours while in the actual implementation, the prediction, aggregation and power allocation are repeated every* 5-15 *minutes in a rolling fashion.*

The result of disaggregation/real-time control using (20) is shown in Figures 5-7. We see that after increasing ψ_b, consumption tracking becomes more important so that user comfort is sacrificed, i.e., temperatures stay at or closely to their lower bounds. We also compare the case of keeping ψ_b unchanged, and it is clear to see the effect of changing weight coefficients from Figure 7. Remark that if the building wants to exactly track the nominal point, $\sum_{i \in \mathcal{G}_F(b)} u_i - p_b^*(b_b - a_b T_b^s) = 0$ can be set as a constraint in (19) rather than appear in the objective function when designing the control. However, doing this may result in infeasibility for problem (19) as discussed in Remark 1.

VI. Conclusion and Future Work

In this paper, an aggregation-disaggregation framework has been developed for building GHP system management in communities. We show how the framework performs, including aggregation of zone information for the future consumption range and utility function of a single building/a group

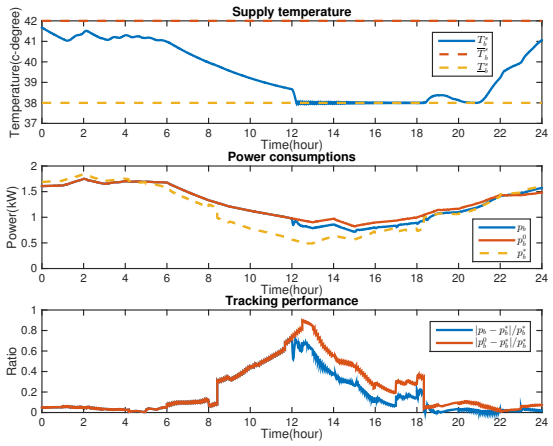

Fig. 7: Disaggregation: trajectories of the supply temperature, power consumptions and tracking performance (superscript '0' denotes the case of using a constant ψ_b all the time).

of buildings, and disaggregation via zone-level distributed control to minimize system efficiency loss. This framework can be scaled up to provide flexible ancillary services to support the power distribution/transmission networks.

Future work will be extending our framework to the management of other types of HVAC systems and home appliances, as well as considering the aggregation/disaggregation problem over multiple time periods. In addition, we are going to study how to formulate proper utility functions and consider their effectiveness and fairness. Last but not least, the physical interaction between the controlled devices and power grids/microgrids will be investigated.

REFERENCES

[1] D. Callaway and I. Hiskens, "Achieving controllability of electric loads," *Proc. IEEE*, vol. 99, no. 1, pp. 184–199, 2011.

[2] UNEP Sustainable Buildings & Climate Initiative, "Buildings and climate change: Summary for decision-makers," *Paris CEDEX 09, France: Sustainable United Nations*, 2009.

[3] B. Yan, "A Bayesian approach for predicting building cooling and heating consumption and applications in fault detection," *PhD dissertation, University of Pennsylvania*, 2013.

[4] F. Tahersima, J. Stoustrup, and H. Rasmussen, "Optimal power consumption in a central heating system with geothermal heat pump," in *Proc. 18th IFAC World Congress*, 2011, pp. 3102–3107.

[5] Z. Yang, G. Pedersen, L. Larsen, and H. Thybo, "Modeling and control of indoor climate using a heat pump based floor heating system," in *Proc. 33rd Annual Conference of the IEEE Industrial Electronics Society*, 2007, pp. 574–579.

[6] R. Halvgaard, N. K. Poulsen, H. Madsen, and J. B. Jørgensen, "Economic model predictive control for building climate control in a smart grid," in *Proc. IEEE PES Innovative Smart Grid Technologies*, 2012.

[7] F. Tahersima, J. Stoustrup, H. Rasmussen, and S. A. Meybodi, "Economic COP optimization of a heat pump with hierarchical model predictive control," in *Proc. of 51st IEEE Conference on Decision and Control*, 2012, pp. 7583–7588.

[8] D. Kirschen and G. Strbac, *Fundamentals of Power System Economics*, 1st ed. John Wiley & Sons, Ltd, 2004.

[9] H. Hao, B. M. Sanandaji, K. Poolla, and T. L. Vincent, "Aggregate flexibility of thermostatically controlled loads," *IEEE Transactions on Power Systems*, vol. 30, no. 1, pp. 189–198, 2015.

[10] W. Mai and C. Y. Chung, "Economic MPC of aggregating commercial buildings for providing flexible power reserve," *IEEE Transactions on Power Systems*, vol. 30, no. 5, pp. 2685–2694, 2015.

[11] S. Grammatico, B. Gentile, F. Parise, and J. Lygeros, "A mean field control approach for demand side management of large populations of thermostatically controlled loads," in *Proc. of 2015 European Control Conference*, 2015, pp. 3548–3553.

[12] L. Zhao and W. Zhang, "A geometric approach to virtual battery modeling of thermostatically controlled loads," in *Proc. of 2016 American Control Conference*, 2016, pp. 1452–1457.

[13] S. J. Crocker and J. L. Mathieu, "Adaptive state estimation and control of thermostatic loads for real-time energy balancing," in *Proc. of 2016 American Control Conference*, 2016, pp. 3557–3563.

[14] N. Li, L. Chen, and S. H. Low, "Optimal demand response based on utility maximization in power networks," in *IEEE Power and Energy Society General Meeting*, 2011.

[15] X. Zhang, W. Shi, Q. Hu, B. Yan, A. Malkawi, and N. Li, "Distributed temperature control via geothermal heat pump systems in energy efficient buildings," in *Proc. of 2017 American Control Conference*, 2017, pp. 754–760.

[16] F. Tahersima, J. Stoustrup, S. A. Meybodi, and H. Rasmussen, "Contribution of domestic heating systems to smart grid control," in *Proc. of 50th IEEE Conference on Decision and Control and European Control Conference*, 2011, pp. 3677–3681.

[17] F. Tahersima, "An integrated control system for heating and indoor climate applications," *PhD dissertation, Aalborg University*, 2012.

[18] Y. Lin, T. Middelkoop, and P. Barooah, "Issues in identification of control-oriented thermal models of zones in multi-zone buildings," in *Proc. of 51st IEEE Conference on Decision and Control*, 2012, pp. 6932–6937.

[19] X. Zhang, W. Shi, B. Yan, A. Malkawi, and N. Li, "Decentralized and distributed temperature control via HVAC systems in energy efficient buildings," *arXiv:1702.03308 [cs.SY]*, 2017.

[20] E. Polymeneas and S. Meliopoulos, "Aggregate modeling of distribution systems for multi-period OPF," in *Proc. 2016 Power Systems Computation Conference*, 2016.

[21] S. Boyd and L. Vandenberghe, *Convex Optimization*. Cambridge University Press, 2004.

[22] X. Zhang and A. Papachristodoulou, "Improving the performance of network congestion control algorithms," *IEEE Transactions on Automatic Control*, vol. 60, no. 2, pp. 522–527, 2015.

[23] X. Zhang, A. Papachristodoulou, and N. Li, "Distributed optimal steady-state control using reverse- and forward-engineering," in *Proc. of 54th IEEE Conference on Decision and Control*, 2015, pp. 5257–5264.

[24] V. Chandan, S. Mishra, and A. G. Alleyne, "Predictive control of complex hydronic systems," in *Proc. of 2010 American Control Conference*, 2010, pp. 5112–5117.

APPENDIX

If the control center is able to allocate power directly, the following problem is solved to derive each p_b^*:

$$\max_{p_b} \sum\nolimits_{b\in\mathcal{G}_F\bigcup\mathcal{G}_R} U_b(p_b) \tag{21a}$$

$$\text{s. t. } \underline{p}_b \le p_b \le \overline{p}_b \tag{21b}$$

$$\underline{p}_c \le \sum\nolimits_{b\in\mathcal{G}_F\bigcup\mathcal{G}_R} p_b \le \overline{p}_c \tag{21c}$$

where $[\underline{p}_c, \overline{p}_c]$ is the range of available power. If the center interacts with the electricity market, an example of the overall utility function is $-\frac{1}{2}(p_c - \sum_{b\in\mathcal{G}_F\bigcup\mathcal{G}_R} p_b^d)^2$ with $\sum_{b\in\mathcal{G}_F\bigcup\mathcal{G}_R} \underline{p}_b \le p_c \le \sum_{b\in\mathcal{G}_F\bigcup\mathcal{G}_R} \overline{p}_b$, where p_c is the overall consumption. The center can use the quadratic curve fitting method as well to generate an overall utility function that minimizes the total Efficiency Loss, given by

$$U_c(p_c) = \alpha_c p_c^2 + \beta_c p_c + \gamma_c \tag{22a}$$

$$U_c\Big(\sum\nolimits_{b\in\mathcal{G}_F\bigcup\mathcal{G}_R} p_b^d\Big) = -\sum\nolimits_{b\in\mathcal{G}_F\bigcup\mathcal{G}_R} EL_b(p_b^d) \tag{22b}$$

$$U_c\Big(\sum\nolimits_{b\in\mathcal{G}_F\bigcup\mathcal{G}_R} \underline{p}_b\Big) = -\sum\nolimits_{b\in\mathcal{G}_F\bigcup\mathcal{G}_R} EL_b(\underline{p}_b) \tag{22c}$$

$$U_c\Big(\sum\nolimits_{b\in\mathcal{G}_F\bigcup\mathcal{G}_R} \overline{p}_b\Big) = -\sum\nolimits_{b\in\mathcal{G}_F\bigcup\mathcal{G}_R} EL_b(\overline{p}_b) \tag{22d}$$

with $\sum_{b\in\mathcal{G}_F\bigcup\mathcal{G}_R} \underline{p}_b \le p_c \le \sum_{b\in\mathcal{G}_F\bigcup\mathcal{G}_R} \overline{p}_b$. Also, weight coefficients can be introduced in (22b)-(22d) when priority of certain buildings is required. Once receiving p_c^* from the market, it solves (21) in which $\underline{p}_c = \overline{p}_c = p_c^*$ to derive p_b^*.